

Estimating Polynomial Structures from Radar Data

Christian Lundquist, Umut Orguner and Fredrik Gustafsson

Linköping University Post Print

N.B.: When citing this work, cite the original article.

©2011 IEEE. Personal use of this material is permitted. However, permission to reprint/republish this material for advertising or promotional purposes or for creating new collective works for resale or redistribution to servers or lists, or to reuse any copyrighted component of this work in other works must be obtained from the IEEE.

Christian Lundquist, Umut Orguner and Fredrik Gustafsson, Estimating Polynomial Structures from Radar Data, 2010, Proceedings of International Conference on Information Fusion.

Postprint available at: Linköping University Electronic Press

<http://urn.kb.se/resolve?urn=urn:nbn:se:liu:diva-62844>

Estimating Polynomial Structures from Radar Data

Christian Lundquist, Umut Orguner and Fredrik Gustafsson

Department of Electrical Engineering

Linköping University

Linköping, Sweden

{lundquist, umut, fredrik}@isy.liu.se

Abstract – *Situation awareness for vehicular safety and autonomy functions includes knowledge of the drivable area. This area is normally constrained between stationary road-side objects as guard-rails, curbs, ditches and vegetation. We consider these as extended objects modeled by polynomials along the road, and propose an algorithm to track each polynomial based on noisy range and bearing detections, typically from a radar. A straightforward Kalman filter formulation of the problem suffers from the errors-in-variables (EIV) problem in that the noise enters the system model. We propose an EIV modification of the Kalman filter and demonstrates its usefulness using radar data from public roads.*

Keywords: extended object, extended target tracking, polynomial, errors in output, errors in variables, automotive radar, road map.

1 Introduction

In classical target tracking problems the objects are modeled as point objects and it is assumed that only one measurement is received from each target at each time step. A target is denoted extended whenever the target extent is larger than the sensor resolution, and it is large enough to occupy multiple resolution cells of the sensor. Put in other words, if a target should be classified as extended does not only depend on its physical size, but rather on the physical size relative to the sensor resolution.

Common methods used to track extended objects are very similar to the ones used for tracking a group of targets moving in formation. Extended object tracking and group tracking are thoroughly described in e.g., [16]. The bibliography in [20] provides a comprehensive overview of existing literature in the area of group and cluster tracking. One conventional method is to model the target as a set of point features in a target reference frame, each of which may contribute at most one sensor measurement. The exact location

of a feature in the target reference frame is often assumed uncertain. The motion of an extended target is modeled through the process model in terms of the translation and rotation of the target reference frame relative to a world coordinate frame, see e.g., [5]. As is the case most of the time, some measurements arise from features belonging to targets and some are due to false detections (clutter). The association hypotheses are derived through some data association algorithm.

Instead of modeling the target as a number of point features, the target may be represented by a spatial probability distribution. It is more likely that a measurement comes from a region of high spatial density than from a sparse region. In [10, 9] it is assumed that the number of received target and clutter measurements are Poisson distributed, hence several measurements may originate from the same target. Each target related measurement is an independent sample from the spatial distribution. The spatial distribution is preferable where the point source models are poor representations of reality, that is, in the cases where the measurement generation is diffuse. In [2], a similar approach is presented, but since raw data is considered, no data association hypotheses are needed.

Objects which are line shaped and curved can often be modeled using polynomials, and tracked as extended targets. Examples of such objects are roads, coast lines, ships and surface topography and these may be tracked from water, ground and aerial vehicles. Typical sensors are radar, laser, sonar and camera. In this paper we consider extended target tracking using polynomials based on radar data, and we apply our ideas to a road mapping scenario using automotive radar sensor reports. In this context, extended targets in the scene can represent guardrails along the road.

This paper is outlined as follows. A basic problem formulation of extended target tracking using polynomials as extended objects is formulated in Section 2. The state space representation that we are going to use in extended target tracking is introduced in Section 3

and simulation results are presented in Section 4. We apply the ideas presented in earlier sections to the road map estimation problem utilizing the automotive radar reports. The experiments done and the results obtained are presented in Section 5. The paper is concluded in Section 6.

2 Problem Formulation

In this paper, we consider target tracking with extended objects that are modeled using n^{th} order polynomials to describe curved lines given as

$$y = a_0 + a_1x + a_2x^2 + \dots + a_nx^n, \quad (1)$$

where a_0, a_1, \dots, a_n are the polynomial coefficients. The state estimates, represented by the coefficients of the polynomial,

$$\mathbf{x} \triangleq [a_0 \quad a_1 \quad \dots \quad a_n]^T, \quad (2)$$

are updated by point measurements from a sensor using standard filters, such as the well known Kalman filter. Suppose we are given the 2-dimensional noisy sensor measurements in batches of Cartesian x and y coordinates as follows.

$$\left\{ \mathbf{z}_k^{(i)} \triangleq [x^{(i)} \quad y^{(i)}]^T_k \right\}_{i=1}^{N_{z_k}}, \quad (3)$$

for discrete time instants $k = 1, \dots, K$. At many cases in reality (e.g., radar, laser and stereo vision) and in the practical application considered in this work, the sensor provides range r and azimuth angle δ given as

$$\left\{ \bar{\mathbf{z}}_k^{(i)} \triangleq [r^{(i)} \quad \delta^{(i)}]^T_k \right\}_{i=1}^{N_{z_k}}. \quad (4)$$

In such a case we assume that some suitable standard polar to Cartesian conversion algorithm is used to convert these measurements into the form (3).

The state models considered in this contribution are described, in general, by the state space equations

$$\mathbf{x}_{k+1} = f(\mathbf{x}_k, \mathbf{u}_k) + \mathbf{w}_k, \quad (5a)$$

$$\mathbf{y}_k = h(\mathbf{x}_k, \mathbf{u}_k) + \mathbf{e}_k, \quad (5b)$$

where \mathbf{x} , \mathbf{u} and \mathbf{y} denotes the state, the input signal, and the output signal, while $\mathbf{w} \sim \mathcal{N}(0, Q)$ and $\mathbf{e} \sim \mathcal{N}(0, R)$ are the process and measurement noise, respectively. The use of a input signal \mathbf{u} is explained in Section 3. For the sake of simplicity, the tracked objects are assumed stationary, resulting in very simple motion models (5a). However, the motion or process model may easily be substituted and chosen arbitrarily to best fit its purpose.

A polynomial is generally difficult to handle in a filter, since the noisy measurements are distributed arbitrarily along the polynomial. In this respect, the measurement models we consider contain parts of the actual measurement vector as parameters. We approach this problem in two ways:

1. In the first method, which we call “errors in output” (EIO), we consider only the errors that are caused by the measurement model output and neglect the errors in the model parameters.
2. The second methodology takes into account also the errors caused by using the actual noisy measurements as model parameters. This scheme is an example of the so called “errors in variables” (EIV) methodology.

The aim is to obtain posterior estimates of the extended source $\mathbf{x}_{k|k}$ given all the measurements $\left\{ \left\{ \mathbf{z}_\ell^{(i)} \right\}_{i=1}^{N_{z_\ell}} \right\}_{\ell=1}^k$ recursively in time. The former approach mentioned above leads to a linear measurement equation and the standard Kalman filter (KF) [12] applies. The second approach, on the other hand, requires a correction in the error statistics of the KF innovations.

As mentioned above, the use of “noisy” measurements as model parameters in this work makes this paper directly related to the errors-in-variables framework, where some of the independent variables are contaminated by noise. Such a case is common in the field of system identification [13] when not only the system outputs, but also the inputs are measured imperfectly. Examples of such EIV representations can be found in [18] and a representative solution is proposed in [11, 7]. The Kalman filter cannot be directly applied to such EIV processes as discussed in [11],[17]. Nevertheless, an extension of the Kalman filter, where the state and the output are optimally estimated in the presence of state and output noise is proposed in [8]. The EIV problem is also closely related to the total-least squares methodology, which is well described in the papers [19, 3, 4], in the survey paper [15] and in the textbook [1].

3 Measurement Model for an Extended Object

This section describes how a point measurement \mathbf{z} relates to the state \mathbf{x} of an extended object. For this purpose, we derive a measurement model in the form (5b), which describes the relation between the state variables \mathbf{x} , defined in (2), and output signals \mathbf{y} and input signals \mathbf{u} . Notice that, for the sake of simplicity, we also drop the subscripts k specifying the time stamps of the quantities.

The general convention in modeling is to make the definitions

$$\mathbf{y} \triangleq \mathbf{z}, \quad \mathbf{u} \triangleq \emptyset, \quad (6)$$

where \emptyset denotes the empty set meaning that there is no input. In this setting, it is extremely difficult, if not impossible, to find a measurement model connecting the outputs \mathbf{y} to the states \mathbf{x} in the form of (5b). Therefore, we are forced to use other selections for \mathbf{y} and \mathbf{u} .

Here, we make the selection

$$\mathbf{y} \triangleq y, \quad \mathbf{u} \triangleq x. \quad (7)$$

Although being quite a simple selection, this choice results in a rather convenient linear measurement model in the state partition \mathbf{x} ,

$$\mathbf{y} = H(\mathbf{u})\mathbf{x} + \mathbf{e}, \quad (8)$$

where $H(\mathbf{u}) = [1 \ x \ x^2 \ \dots \ x^n]^\top$. It is the selection in (7) rather than (6) that allows us to use the standard methods in target tracking with clever modifications. Such a selection as (7) is also in accordance with the errors-in-variables representations where measurement noise are present in both the outputs and inputs, i.e., the observation \mathbf{z} can be partitioned according to

$$\mathbf{z} = \begin{bmatrix} \mathbf{u} \\ \mathbf{y} \end{bmatrix}. \quad (9)$$

We express the measurement vector given in (3) in terms of a noise free variable \mathbf{z}_0 which is corrupted by additive measurement noise $\tilde{\mathbf{z}}$ according to

$$\mathbf{z} = \mathbf{z}_0 + \tilde{\mathbf{z}}, \quad \tilde{\mathbf{z}} \sim \mathcal{N}(0, \Sigma_c), \quad (10)$$

where the covariance Σ_c can be decomposed as

$$\Sigma_c = \begin{bmatrix} \Sigma_x & \Sigma_{xy} \\ \Sigma_{xy} & \Sigma_y \end{bmatrix}. \quad (11)$$

Note that, in the case the sensor provides measurements only in polar coordinates (4), one has to convert both the measurement $\tilde{\mathbf{z}}$ and the measurement noise covariance

$$\Sigma_p = \text{diag}(\sigma_d^2, \sigma_\delta^2) \quad (12)$$

into Cartesian coordinates. This is a rather standard procedure and one simple method is described in the Appendix. Note that, in such a case, the resulting Cartesian measurement covariance Σ_c is, in general, not necessarily diagonal and hence Σ_{xy} of (11) might be non-zero.

Since the model (8) is linear, the Kalman filter measurement update formulas can be used to incorporate the information in \mathbf{z} into the extended source state \mathbf{x} . An important question in this regard is what would be the measurement covariance of the measurement noise term \mathbf{e} in (8). This problem can be tackled in two ways, which are described in the Section 3.1 and 3.2.

3.1 Errors in Output (EIO) Scheme

Although the input terms defined in (7) are measured quantities (and hence affected by the measurement noise), and therefore the model parameters $H(\mathbf{u})$ are uncertain, in a range of practical applications where parameters are obtained from measurements, such errors are neglected. Thus, the first scheme we present

here neglects all the errors in $H(\mathbf{u})$. In this case, it can easily be seen that

$$\mathbf{e} = \tilde{\mathbf{y}} \quad (13)$$

and therefore the covariance Σ of \mathbf{e} is

$$\Sigma = \Sigma_y. \quad (14)$$

This type of approach was also used in our previous work [14] which presented earlier versions of the findings in this paper.

3.2 Errors in Variables (EIV) Scheme

Neglecting the errors in the model parameters $H(\mathbf{u})$ can cause overconfidence in the estimates of recursive filters and can actually make data association difficult in tracking applications (by causing too small gates). We, in this second scheme, use a simple methodology to take the uncertainties in $H(\mathbf{u})$ into account in line with the EIV framework. Assuming that the elements of the noise free quantity \mathbf{z}_0 satisfy the polynomial equation exactly, we get

$$\mathbf{y} - \tilde{\mathbf{y}} = H(\mathbf{u} - \tilde{\mathbf{u}})\mathbf{x}, \quad (15a)$$

$$\mathbf{y} - \tilde{\mathbf{y}} = [1 \ x - \tilde{x} \ (x - \tilde{x})^2 \ \dots \ (x - \tilde{x})^n] \mathbf{x}, \quad (15b)$$

which can be approximated using a first order Taylor expansion resulting in

$$\mathbf{y} \approx H(\mathbf{u})\mathbf{x} - \tilde{H}(\mathbf{u})\tilde{x}\mathbf{x} + \tilde{\mathbf{y}} \quad (16a)$$

$$= H(\mathbf{u})\mathbf{x} + \tilde{h}(\mathbf{x}, \mathbf{u}) \begin{bmatrix} \tilde{x} \\ \tilde{y} \end{bmatrix}, \quad (16b)$$

with

$$H(\mathbf{u}) = [1 \ x \ x^2 \ \dots \ x^n], \quad (16c)$$

$$\tilde{H}(\mathbf{u}) = [0 \ 1 \ 2x \ \dots \ nx^{n-1}], \quad (16d)$$

$$\tilde{h}(\mathbf{x}, \mathbf{u}) = [-a_1 - 2a_2x - \dots - na_nx^{n-1} \ 1]. \quad (16e)$$

Hence, the noise term \mathbf{e} of (8) is given by

$$\mathbf{e} = \tilde{\mathbf{y}} - \tilde{H}\tilde{x}\mathbf{x} = \tilde{h}(\mathbf{x}, \mathbf{u}) \begin{bmatrix} \tilde{x} \\ \tilde{y} \end{bmatrix} \quad (17)$$

and its covariance is given by

$$\begin{aligned} \Sigma &= E(\mathbf{e}\mathbf{e}^\top) = \Sigma_y + \mathbf{x}^\top \tilde{H}^\top \Sigma_x \tilde{H} \mathbf{x} - 2\tilde{H} \Sigma_{xy} \\ &= \tilde{h}(\mathbf{x}, \mathbf{u}) \Sigma_c \tilde{h}(\mathbf{x}, \mathbf{u}). \end{aligned} \quad (18)$$

Note that the EIV covariance Σ depends on the state variable \mathbf{x} , which is substituted by its last estimate in recursive estimation.

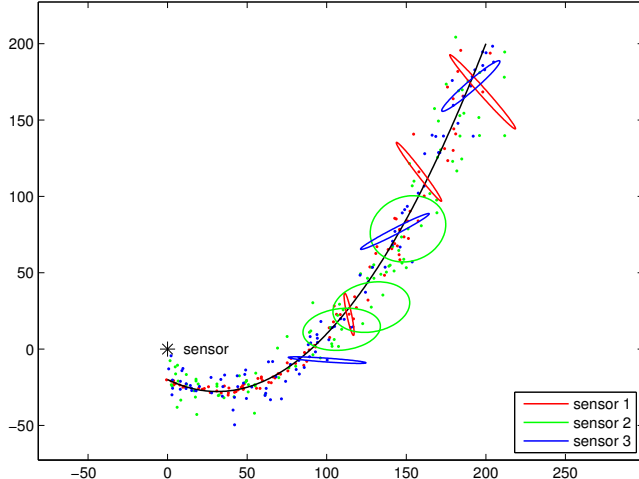


Figure 1: The true polynomial and the extracted measurements are shown. Covariance ellipses are drawn for a few measurements to show the direction of the uncertainties.

4 Simulation Example

A simulation example is used to compare the performances of the EIO and the EIV schemes. The MATLAB code used to produce the simulations and figures in this paper is available online¹. A second order polynomial with the true states

$$\mathbf{x} = [a_0 \quad a_1 \quad a_2]^T = [-20 \quad -0.5 \quad 0.008]^T \quad (19)$$

is used and 100 uniformly distributed measurements are extracted in the range $x = [0, 200]$. The measurements are given on polar form as in (4) and zero mean Gaussian measurement noise with covariance as in (12) is added using the parameters

$$\text{Sensor 1:} \quad \sigma_{d1} = 0.5, \quad \sigma_{\delta 1} = 0.05, \quad (20a)$$

$$\text{Sensor 2:} \quad \sigma_{d2} = 10, \quad \sigma_{\delta 2} = 0.05, \quad (20b)$$

$$\text{Sensor 3:} \quad \sigma_{d3} = 10, \quad \sigma_{\delta 3} = 0.005, \quad (20c)$$

to simulate different type of sensors. Sensor 1 represents a sensor with better range than bearing accuracy, whereas the opposite holds for sensor 3. Sensor 2 has about the same range and bearing accuracies. The true polynomial and the measurements are shown in Figure 1. The measurements are transformed into Cartesian coordinates as described in the Appendix. The following batch methods ($N_{z_k} = 100$, $K = 1$) are applied to estimate the states

- Least squares (LS EIO) estimator,
- Weighted least squares (WLS EIO) with EIO covariance,
- Weighted least squares (WLS EIV) with EIV covariance. The state \mathbf{x} used in (18) is estimated through a least squares solution in advance.

Furthermore, the states are estimated recursively ($N_{z_k} = 1$, $K = 100$) using

- Kalman filter (KF EIO) with EIO covariance,
- Kalman filter (KF EIV) with EIV covariance. The predicted state estimate $\hat{\mathbf{x}}_{k|k-1}$ is used in (18) to derive R_k .
- Unscented Kalman filter (UKF EIV) with sigma points derived by augmenting the state vector with the noise terms

$$\tilde{\mathbf{z}} = [\tilde{\mathbf{u}} \quad \tilde{\mathbf{y}}]^T, \quad \tilde{\mathbf{z}} \sim \mathcal{N}(0, \Sigma_c), \quad (21)$$

to consider the error in all directions (as in the EIV case), and to deal with the nonlinear transformations of the noise terms. The sigma points are propagated through the nonlinear polynomial equation (15), i.e.,

$$\mathbf{y} = H(\mathbf{u} - \tilde{\mathbf{u}})\mathbf{x} + \tilde{\mathbf{y}}. \quad (22)$$

The covariance of the process noise is set to zero, i.e., $Q = 0$, since the target is not moving. The initial conditions of the state estimate are selected as

$$\hat{\mathbf{x}}_0 = [0 \quad 0 \quad 0]^T, \quad (23a)$$

$$P_0 = \left(\frac{\sigma^2}{\kappa} \text{diag}(\mathbf{x}) \right)^2, \quad (23b)$$

where $\kappa = 3$ and $\sigma^2 = 8$. Note that every estimate's initial uncertainty is set to be a scaled version of its true value in (23b).

The RMSE values for 1000 Monte Carlo simulations are given in Table 1. The RMSE of the EIV schemes is clearly lower than the other methods, especially for sensor 1 and 3 with non-symmetric measurement noise. This result justifies the extra computations required for calculating the EIV covariance. There is only a small difference in the performance between the KF EIV and the UKF EIV for the second order polynomial. This is a clear indication of that the simple Taylor series approximation used in deriving the EIV covariance is accurate enough.

5 Experiments using Radar Measurements

Guardrails along the roads are shaped as curved lines, and in the framework of this work, they can be tracked as extended objects. To show this, we use noisy radar reports from a passenger car, collected during driving on a Swedish freeway. The measurements are collected from a moving vehicle and are transformed from the vehicle's frame to the common world frame. The experiment here is conducted in two steps; first a ground truth (reference) value for the state \mathbf{x} is found by manually removing clutter and outliers, and thereafter the

¹www.control.isy.liu.se/publications/doc?id=2300

Table 1: RMSE values for the extended object in Figure 1. The sensor configurations are defined in (20).

Sensor		LS	WLS	WLS	KF	KF	UKF
		EIO	EIO	EIV	EIO	EIV	EIV
1	a_0	5.10	0.55	0.45	0.55	0.48	0.49
	a_1	0.18	0.034	0.024	0.034	0.029	0.029
	a_2 (10^{-3})	1.06	0.29	0.24	0.29	0.31	0.32
2	a_0	4.90	3.54	3.35	2.90	2.44	2.36
	a_1	0.20	0.11	0.099	0.10	0.11	0.10
	a_2 (10^{-3})	1.21	0.77	0.66	0.78	0.83	0.80
3	a_0	2.53	30.51	3.51	30.47	4.81	4.35
	a_1	0.068	0.45	0.072	0.45	0.12	0.12
	a_2 (10^{-3})	0.39	1.27	0.40	1.26	0.62	0.60

Table 2: The RMSE values are given as the error of the filtered state estimates of the guardrail compared with the smoothed and clutter-free reference.

	KF	KF	UKF
	EIO	EIV	EIV
a_0	0.20	0.13	0.10
a_1 (10^{-3})	4.44	3.60	3.31
a_2 (10^{-6})	11.47	9.57	8.49

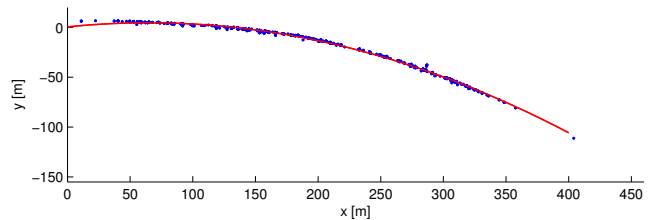
states are estimated using the complete set of measurements.

We choose one guardrail from a sequence of measurement, which is used to exemplify the methods. One piece of this guardrail is shown on the left hand side of the road in Figure 2a. All measurements in the time sequence $k = 1, \dots, K = 147$ stemming from this guardrail are used to estimate the polynomial coefficients. Measurements were checked manually and outliers are removed to obtain the ground truth for comparing estimates. The ground truth line, shown as the red line in Figure 2b, is given by the solution of a least squares problem, taking the radar measurements, shown as blue dots in Figure 2b, as input.

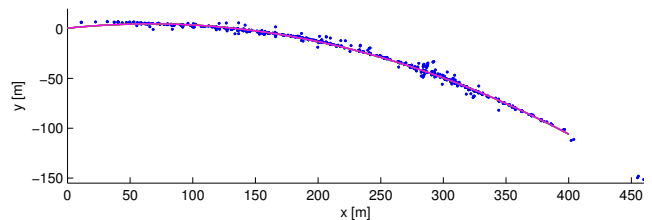
After having found the reference values of \mathbf{x} , the state estimates are estimated recursively for each time instant k . That means that we compare the filtered values for each time step $k = 1, \dots, 147$ with the smoothed estimate. All radar measurements, including clutter, are used, as can be seen in Figure 2c, where the blue dots illustrates the radar measurements. As in the previous sections we compare the EIO KF, the EIV KF and the EIV UKF. The results are very similar and the colored lines in Figure 2c are not distinguishable. The resulting RMSE values are presented in Table 2, and these results are basically in line with the results of the simulation example in the previous section, i.e. the errors of the EIV methods are lower than the errors of the EIO method.



(a)



(b)



(c)

Figure 2: A traffic situation is shown in Figure (a) and the guardrail on the left side provides a line shaped extended target in this example. A reference value is obtained by using the clutter-free measurements in Figure (b) and the filtered results are given using all data in Figure (c).

Roads can only be modeled locally using polynomials, see e.g., [6]. In [14] we show how to estimate several local polynomials including start and end points along the road.

6 Conclusion

In this contribution we have considered the use of polynomials in extended target tracking. Measurement models that enables the use of Kalman filters for the polynomial shaped extended objects are introduced. Simulation examples show the advantage of utilizing errors-in-variable methods for this type of problems. The approach has also been evaluated for tracking a guardrail, based on real radar data collected on a Swedish freeway.

Acknowledgment

The authors would like to thank the Linnaeus center CADICS, funded by the Swedish Research Council and the strategic research center MOVIII, funded by the Swedish Foundation for Strategic Research (SSF) for financial support.

Appendix

The measurement vector \mathbf{z} expressed using polar coordinates and the corresponding measurement covariance $\Sigma_p = \text{diag}(\sigma_d, \sigma_\delta)$ are first transformed to Cartesian coordinates. The covariance is derived by differential analysis using small error terms denoted Δ , using any nonlinear method, e.g. a first order Taylor expansion according to

$$\begin{bmatrix} x^{E_s} \\ y^{E_s} \end{bmatrix} = \begin{bmatrix} (d\Delta d) \cos(\delta + \Delta\delta) \\ (d\Delta d) \sin(\delta + \Delta\delta) \end{bmatrix} \quad (24a)$$

$$= \begin{bmatrix} d \cos \delta \\ d \sin \delta \end{bmatrix} + \underbrace{\begin{bmatrix} \cos \delta & -d \sin \delta \\ \sin \delta & d \cos \delta \end{bmatrix}}_{\triangleq A_1} \begin{bmatrix} \Delta d \\ \Delta \delta \end{bmatrix}. \quad (24b)$$

The resulting Cartesian coordinates of the measurements expressed in the sensors coordinate frame E_s are

$$\mathbf{z}^{E_s} = \begin{bmatrix} x^{E_s} \\ y^{E_s} \end{bmatrix} = \begin{bmatrix} d \cos \delta \\ d \sin \delta \end{bmatrix}, \quad (25)$$

and the measurement covariance is $\Sigma_c = A_1 \Sigma_p A_1^T$.

References

[1] Å Björck. *Numerical methods for least squares problems*. SIAM, Philadelphia, PA, USA, 1996.

[2] Y. Boers, H. Driessen, J. Torstensson, M. Trieb, R. Karlsson, and F. Gustafsson. Track-before-detect algorithm for tracking extended targets. In *IEE Proceedings on Radar and Sonar Navigation*, volume 153, pages 345–351, 2006.

[3] D. L. Boley and K. Sutherland. Recursive total least squares: An alternative to the discrete kalman filter. In *AMS Meeting on Applied Linear Algebra 882*, May 1993.

[4] B. De Moor. Structured total least-squares and l_2 approximation-problems. *Linear algebra and its applications*, 188-189:163–207, 1993.

[5] J. C. Dezert. Tracking maneuvering and bending extended target in cluttered environment. In *Proceedings of Signal and Data Processing of Small Targets*, volume 3373, pages 283–294. SPIE, 1998.

[6] E. D. Dickmanns. *Dynamic Vision for Perception and Control of Motion*. Springer, London, UK, 2007.

[7] R. Diversi, R. Guidorzi, and U. Soverini. Algorithms for optimal errors-in-variables filtering. *Systems & Control Letters*, 48(1):1–13, 2003.

[8] R. Diversi, R. Guidorzi, and U. Soverini. Kalman filtering in extended noise environments. *IEEE Transactions on Automatic Control*, 50(9):1396–1402, September 2005.

[9] K. Gilholm, S. Godsil, S. Maskell, and D. Salmond. Poisson models for extended target and group tracking. In Oliver E. Drummond, editor, *Proceedings of Signal and Data Processing of Small Targets*, volume 5913. SPIE, 2005.

[10] K. Gilholm and D. Salmond. Spatial distribution model for tracking extended objects. In *IEE Proceedings of Radar, Sonar and Navigation*, volume 152, pages 364–371, October 2005.

[11] R. Guidorzi, R. Diversi, and U. Soverini. Optimal errors-in-variables filtering. *Automatica*, 39(2):281–289, 2003.

[12] R. E. Kalman. A new approach to linear filtering and prediction problems. *Transactions of the ASME, Journal of Basic Engineering*, 82:35–45, 1960.

[13] L. Ljung. *System identification, Theory for the user*. System sciences series. Prentice Hall, Upper Saddle River, NJ, USA, second edition, 1999.

[14] C. Lundquist, U. Orguner, and T. B. Schön. Tracking stationary extended objects for road mapping using radar measurements. In *Proceedings of the IEEE Intelligent Vehicles Symposium*, pages 405–410, Xi'an, China, June 2009.

[15] I. Markovsky and S. van Huffel. Overview of total least-squares methods. *Signal Processing*, 87(10):2283 – 2302, 2007. Special Section: Total Least Squares and Errors-in-Variables Modeling.

- [16] B. Ristic, S. Arulampalam, and N. Gordon. *Beyond the Kalman Filter: Particle filters for tracking applications*. Artech House, London, UK, 2004.
- [17] B. Roorda and C. Heij. Global total least squares modeling of multivariable time series. *IEEE Transactions on Automatic Control*, 40(1):50–63, January 1995.
- [18] T. Söderström. Survey paper: Errors-in-variables methods in system identification. *Automatica*, 43(6):939–958, 2007.
- [19] S. van Huffel and H. Zha. An efficient Total Least Squares algorithm based on a rank-revealing two-sided orthogonal decomposition. *Numerical Algorithms*, 4:101–133, February 1993.
- [20] M. J. Waxman and O. E. Drummond. A bibliography of cluster (group) tracking. In *Proceedings of Signal and Data Processing of Small Targets*, volume 5428, pages 551–560. SPIE, 2004.